Performance Evaluation of the ISS Water Processor Multifiltration Beds

Elizabeth M. Bowman, Ph.D.[1]
The Boeing Company, Huntsville, Alabama, 35806

Layne Carter[2]
NASA Marshall Space Flight Center, Huntsville, Alabama, 35812

Mark Wilson[3]
The Boeing Company, Houston, Texas, 77059

Harold Cole[4]
The Boeing Company (retired), Huntsville, Alabama, 35806

Nicole Orozco[5]
The Boeing Company, Houston, Texas, 77058

and

Douglas Snowdon[6]
Hamilton Sundstrand, Windsor Locks, CT, 06096

The ISS Water Processor Assembly (WPA) produces potable water from a waste stream containing humidity condensate and urine distillate. The primary treatment process is achieved in the Multifiltration Bed, which includes adsorbent media and ion exchange resin for the removal of dissolved organic and inorganic contaminants. The first Multifiltration Bed was replaced on ISS in July 2010 after initial indication of inorganic breakthrough. This bed was returned to ground in July 2011 for an engineering investigation. The water resident in the bed was analyzed for various parameters to evaluate adsorbent loading, performance of the ion exchange resin, microbial activity, and generation of leachates from the ion exchange resin. Portions of the adsorbent media and ion exchange resin were sampled and subsequently desorbed to identify the primary contaminants removed at various points in the bed. In addition, an unused Multifiltration Bed was evaluated after two years in storage to assess the generation of leachates during storage. This assessment was performed to evaluate the possibility that these leachates are impacting performance of the Catalytic Reactor located downstream of the Multifiltration Bed. The results of these investigations and implications to the operation of the WPA on ISS are documented in this paper.

[1] Lead Chemist, Boeing Huntsville Laboratories, 499 Boeing Blvd, JW-56, Huntsville, AL 35824, Senior Member.
[2] Life Support Development Team Lead, NASA, MSFC ES62, Huntsville, AL 35812, Senior Member.
[3] Associate Technical Fellow, Boeing Research & Technology, 13100 Space Center Blvd., MC HB3-20, Houston, TX 77059, Senior Member.
[4] Associate Technical Fellow (retired), Boeing Huntsville Laboratory, 499 Boeing Blvd, JW-56, Huntsville, AL 35824.
[5] Water Processor Assembly / Water Recovery & Management Subsystem Lead, Environmental Control and Life Support, 3700 Bay Area Blvd., Houston, TX 77059.
[6] Principal Engineer, Space, Land, and Sea, Hamilton Sundstrand, Windsor Locks, CT, 06096.

Nomenclature

ISS = International Space Station
WPA = Water Processor Assembly
MF Bed = Multifiltration Bed
TOC = Total Organic Carbon
TIC = Total Inorganic Carbon
TOCA = Total Organic Carbon Analyzer
ICP-OES = Inductively Coupled Plasma-Optical Emission Spectroscopy
IC = Ion Chromatograph
DMSD = dimethylsilanediol
VFA = Volatile Fatty Acid
NTU = Nephelometric Turbidity Units
ppm = Parts per Million, equivalent to mg/L
mg/L = milligrams per liter
ppb = Parts per Billion, equivalent to µg/L
µg/L = micrograms per liter
SEM/EDXRF = Scanning Electron Microscopy with Energy Dispersive X-Ray Fluorescence detector
mL = milliliter
µm = micrometer
mm = millimeter
CFU = colony forming units
MIS = Microbial Identification System
g = gram
GNR = Gram negative rod
TNTC = too numerous to count

I. Introduction

The International Space Station (ISS) Water Processor Assembly (WPA) was initially activated in November of 2008 and is used to produce potable water from humidity condensate, Urine Processor Assembly (UPA) distillate, and Sabatier product water. The ISS WPA has been described and reported on elsewhere.[1] This paper will focus on a key technology of the WPA, which is the use of Multifiltration (MF) Beds that use adsorbent media and ion exchange resins to remove dissolved organic and inorganic contaminants. Two MF Beds in the WPA are used in series, with a conductivity sensor between them to monitor for the breakthrough of ionic contaminants through the first bed. Effluent from the MF Beds is further processed through a Catalytic Reactor to oxidize low molecular weight organics that are not efficiently removed by the MF Bed adsorbents. A Total Organic Carbon Analyzer (TOCA) provides weekly analysis of the WPA product water quality.

Between June and November of 2010, on orbit TOCA measurements showed steadily increasing concentrations of Total Organic Carbon (TOC) in the WPA product water. Analysis of the product water identified dimethylsilanediol (DMSD) as the primary contributor to the rise in TOC[1]. Prior to identifying DMSD, the decision was made to replace both MF Beds to address the concern that a larger organic contaminant was passing through the MF Bed and impacting reactor performance. This maintenance activity occurred on July 29, 2010. At the time the beds were replaced, on-orbit conductivity data indicated initial ionic breakthrough of the first MF Bed had occurred. The MF Beds were then stored on orbit for several months, returned to ground, and stored again for several months. In August and September of 2011, MF Bed S/N 00003, which was the first bed in line in the WPA on orbit, was shipped and sampled at Hamilton Sundstrand. Samples included water and resin samples from each of the ten tubes that comprise the single MF Bed. Samples were sent to various laboratories for analysis, including Hamilton Sundstrand (where sampling occurred) and Boeing Huntsville Laboratories. Analysis results and their implications with respect to MF Bed life and capacity are discussed in this paper.

II. Sampling of Multifiltration Bed S/N 03

MF Bed S/N 03 was received at Hamilton Sundstrand's facility in August, 2011. The MF Bed consists of ten tubes (Fig. 1), with the first three tubes containing adsorbent and the last seven tubes containing ion exchange resin. Once the tubes were opened, approximately 1 L of water was drained out of each tube and samples were collected serially. One sample was collected into a sterile 50 mL centrifuge tube for microbiological analysis (BHL), and four others were collected for chemical analysis (HS and BHL). After draining the water, the resin from each tube was

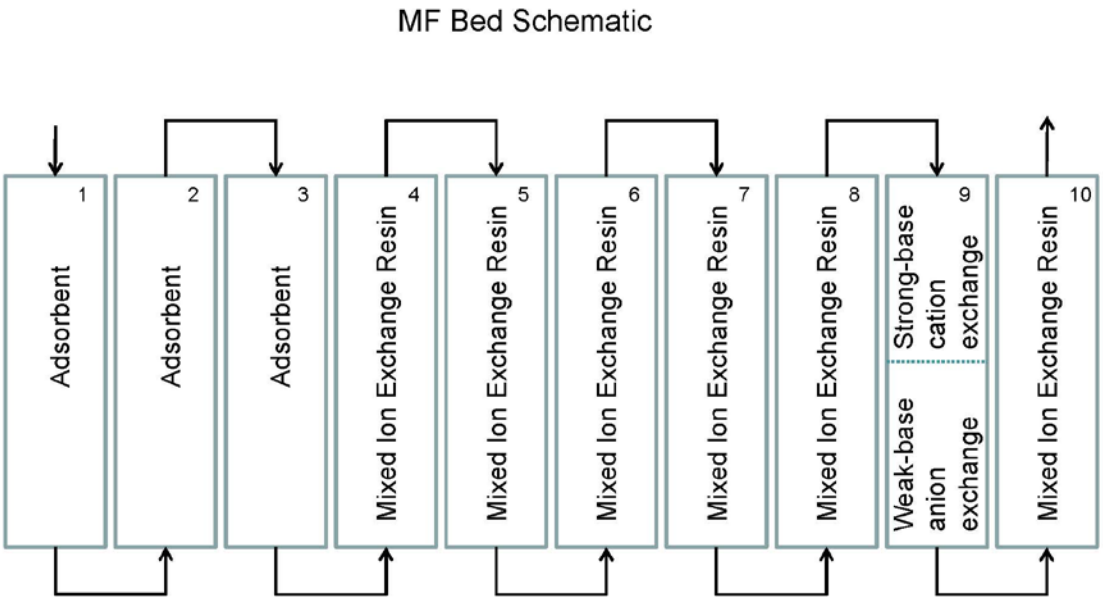

Figure 1. MF Bed schematic showing tube numbers, flow paths, and resin types.

sampled as it was pushed out of the tube. Resin samples for microbiological analyses were initially collected into a sterile 15 mL centrifuge tube containing 5 mL of neutralizing buffer. Resin samples for chemical analyses were collected from the inlet, middle, outlet, or as a composite, depending on the tube, type of resin, and scheduled analyses. Additionally, tube 9, which includes a split of cation exchange resin and weak base anion exchange resin, was flushed several times and the flush water collected for analysis. This paper will discuss analysis results in terms of tube number (1-10) for either water or resin samples.

The analysis plan for water samples included identification and measurement of inorganic (pH, conductivity, Total Inorganic Carbon [TIC], inorganic ions) and organic (TOC, semivolatiles, and volatiles) compounds, microbial count and identification, and fungal count and identification. Analysis plans for resin samples focused on identification and measurement of inorganic and organic compound loading as well as microbial count and identification and fungal count and identification.

During sampling, the change in sorbent bed length in each tube was measured. For many resins, this can be related to the amount of material sorbed onto the resin. The increase in sorbent bed length for each tube is shown in Table 1. The first three sorbents are carbon and experience little change in sorbent bed length, which is expected given that carbon has little elasticity to expand or contract. Tubes 4 through 8, however, show a trend with tube 4 having contracted the most and tube 8 the least. This is consistent with the expectation for contraction or shrinkage on use of the mixed cation/anion exchange resin used in tubes 4 through 8. Tube 4, being the first ion exchange resin tube, should adsorb the most ions and therefore shrink the most. In contrast, tube 9 shows an increase in resin bed length. Tube 9 has two different resins in it, one of which expands during use and one that contracts during use. The measured increase is inconclusive by itself because is it could be a combination of both expansion and contraction for the two different resins. It does certainly indicate that the resin that expandss (the weak base anion exchange resin) had some sorption, but it is impossible from this data alone to compare the two resins in tube 9 in terms of sorbent bed length changes. Tube 10 sorbent bed length increase is not available due to hardware constraints.

Table 1. Decrease in bed length in inches for each tube in MF Bed.

Tube number	Increase in sorbent bed length, inches
1	0.142
2	0.084
3	0.044
4	-2.305
5	-2.248
6	-2.037
7	-2.072
8	-1.423
9	+0.795
10	not available

III. Analysis Approach

Table 2 shows the analyses planned for each sample type. For select water samples, Fourier Transform Infrared (FTIR) spectroscopy, Scanning Electron Microscopy with Energy Dispersive X-Ray Fluorescence detector (SEM/EDXRF), and visual inspection were used to further characterize some components.

Table 2. Sample analysis plan.

Tube Number	Sample Type	Analyses
1 through 10	Water	pH TIC/TC Turbidity Total and Dissolved Metals Ammonium Ion (as Total Ammonia) Inorganic Anions Volatile Organic Compounds Semivolatile Organic Compounds Volatile Fatty Acids Microbial Count and ID Fungal Count and ID
1 through 3	Carbon Adsorbent (desorbed with methanol and dichloromethane)	Semivolatile Organic Compounds Microbial Count and ID Fungal Count and ID
4 through 10	Ion Exchange Resin (desorbed with 0.5 N acid and base)	Total and Dissolved Metals Ammonium Ion (as Total Ammonia) Inorganic Anions Semivolatile Organic Compounds Volatile Organic Compounds Volatile Fatty Acids Microbial Count and ID Fungal Count and ID

For chemical analysis, all sorbent samples were desorbed using appropriate liquid phases, and the desorbates were analyzed. For tubes 1 through 3 (carbon adsorbent), methanol and dichloromethane were used to desorb analytes. Semivolatiles were measured in the carbon desorbates. Analyses of the ion exchange resin desorbates (tubes 4 through 10) analysis are listed in Table 2. The scheme for ion exchange resin desorption, extraction of semivolatiles, and desorbate analysis is shown in Figure 2. Metals were measured by Inductively Coupled Plasma / Optical Emission Spectrometry (ICP/OES), ammonium ion was measured as total ammonia by an UltraViolet-Visible (UV-Vis) spectroscopy method, and inorganic anions were measured by Ion Chromatography (IC). Semivolatiles in acid extract (base / neutral fraction and acid / neutral fraction), semivolatiles in base extract (base / neutral fraction and acid / neutral fraction), volatile fatty acids in base extract, and volatiles in water were all measured by Gas Chromatography – Mass Spectrometry (GC-MS).

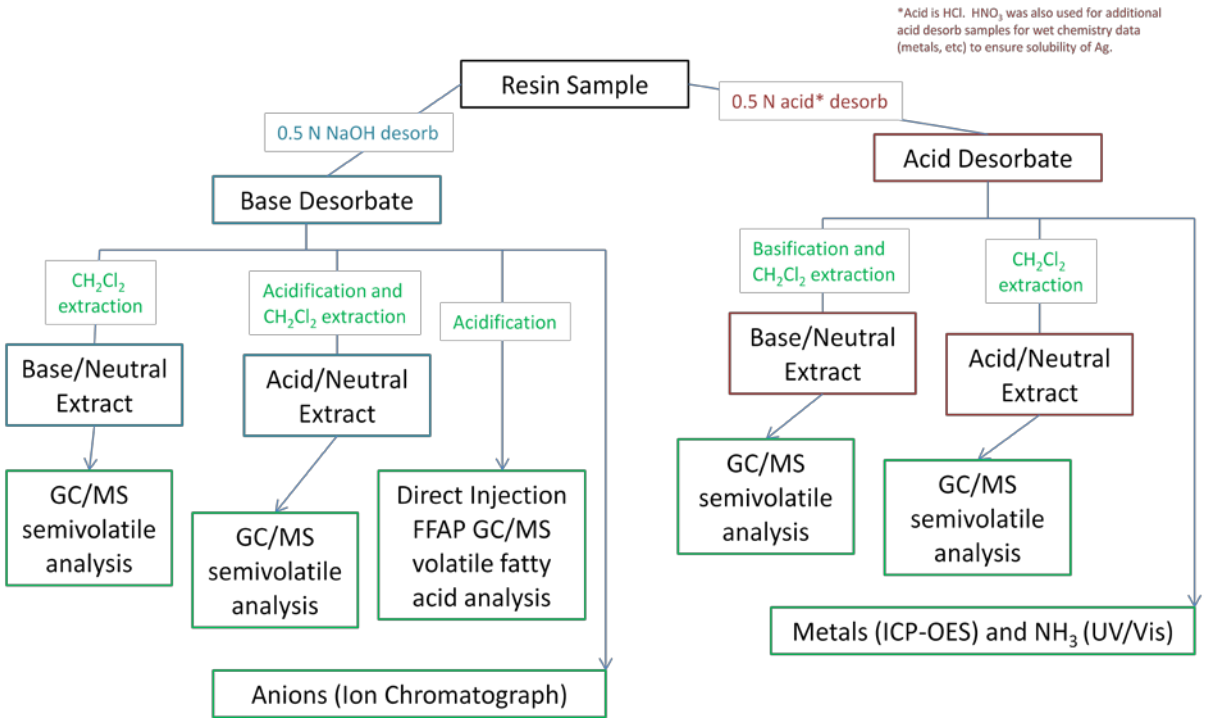

Figure 2. Ion exchange resin desorption and analysis schematic.

Microorganisms were dispersed from the carbon or resin samples into the neutralizing buffer by three repetitions of vortexing for 30 seconds followed by sonication for 1 minute. Microbiological enumerations of heterotrophic bacteria and fungi in water and neutralizing buffer carbon/resin samples were performed by membrane filtration.[4] Dilutions for each sample were prepared using 1 mL water or neutralizing buffer in 99 mL sterile phosphate buffered saline and each dilution was filtered in duplicate through 0.45 µm, gridded, 47 mm Millipore HAWG sterile filters and placed onto R2A agar for heterotrophic bacteria, and then incubated for 7 days at 28°C. The membrane filters for fungi were placed on modified Emmon's Agar, which contains chloramphenicol and rose bengal to inhibit bacterial growth, and then incubated for 5 days at 25°C. Counts of bacteria and fungi were reported as colony forming units (CFU)/mL for water or CFU/g for the carbon and resin samples. Bacteria identifications were performed using the Sherlock® Microbial Identification System (MIS) which is based on cellular fatty acid analysis by gas chromatography. Bacteria identifications were also performed using the Biolog MicroLog Identification System that is based on carbon source utilization patterns within a 96 well microplate using oxidation-reduction chemistry.

IV. Analysis Results

Chemical and microbial analysis results are presented here in terms of tube number (1 through 10) for both water and resin samples. Note that tube nine contains two separate resins; those resin samples are numbered 9 and 9.5 for clarity and ease of comparison with water data.

A. Wet Chemical Analysis of Water and Sorbent (Resin) Samples

Wet chemical analysis includes all inorganic analyses as well as pH, conductivity, TIC, and TOC. Some parameters, such as pH, are affected by organic compounds and the organic analytical data is referenced for the reader where appropriate.

Figure 3 shows the variance of conductivity and pH with tube number through the MF Bed. Note that the pH ranges between 6.2 and 6.8 for tubes 1 through 6 and then drops below 4 in tubes 7 and 8. The pH rises back up in tube 9 and drops again in tube 10. The pH drop after tube 6 is coincident with the absence of ammonium ion (Fig. 4). Data also show that while volatile fatty acids (VFAs) are low in tube 1 through 6 (Fig. 20), the VFA concentration rises in tubes 7 and 8 and peaks in tube 9. The absence of ammonium and the presence of high VFAs are most likely responsible for the pH drop in tubes 7 and 8. The higher pH in tube 9 is due to the presence of N,N-dimethyl-1,3-propanediamine (Fig. 17-18), which is a degradation product of one of the resins in tube 9. Also shown in Figure 3, conductivity steadily decreases through the MF Bed water samples, reflecting the loading of ions on the resins. However, there is a sharp increase in conductivity in the tube 9 water, primarily due to the combined presence of N,N-dimethyl-1,3-propanediamine and acetic acid, which are likely present as a dissolved ionic salt.

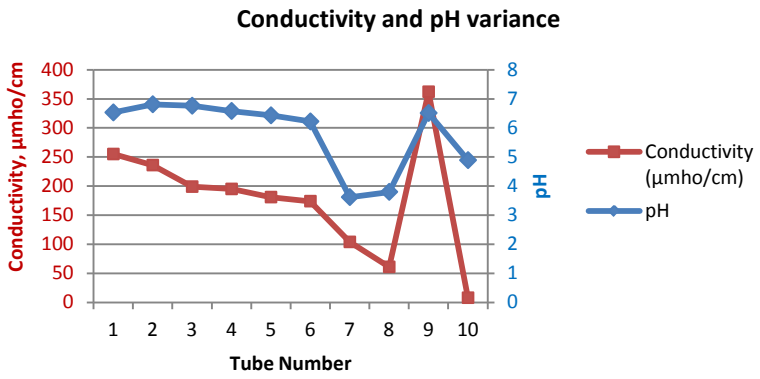

Figure 3. Conductivity and pH variance in water samples.

Figure 4 shows the concentration of inorganic cations in the MF Bed water samples from tubes 1 through 10. In Figure 4, the blue line represents the total concentration of inorganic cations (metals plus ammonium ion) in the water, the green line represents the concentration of ammonium ion in water, and the red line represents total metals in water, all in mg/L. Ammonium ion is adsorbed on the ion exchange resin primarily in tubes 4 through 6, after the metals are adsorbed. Cation exchange resins generally have a stronger affinity for metals than for ammonium ion, so this result is expected. Because the amount of cations is very low in tubes 7 through 10, it is clear that the MF Bed is not saturated and there is still remaining capacity with respect to cations.

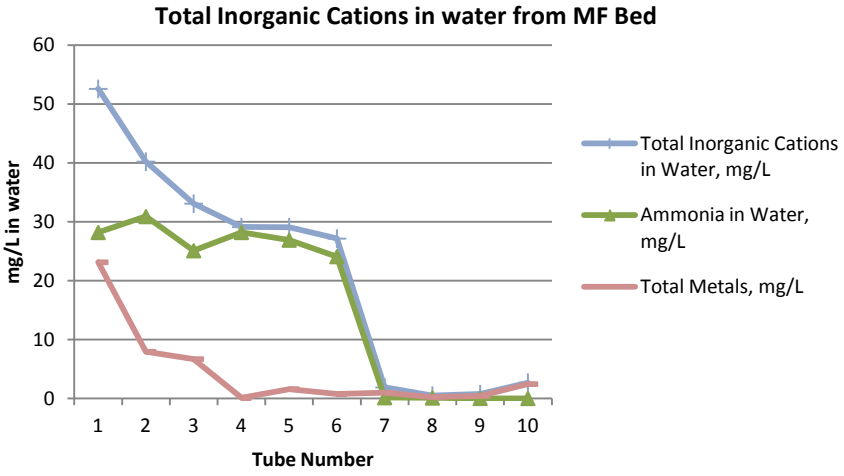

Figure 4. Inorganic cation concentrations measured in water.

Figure 5 shows the loading of ammonia and

metal ions on the ion exchange resins sampled from tubes 4 through 10 in micrograms of cation per gram of resin (µg/g) as calculated from measured concentrations in the acid desorbates. In tube 4, it is clear that the last of the metal cations are adsorbed onto the resin, allowing only a limited amount of ammonium loading. In tubes 5 through 7 where there is little or no competition from metal cations for the sorption sites, the ammonium ion is removed. The data from the resin desorption (Figure 5) agree with the data from the water (Figure 4) in that the metal cations are almost all removed before tube 5 and the ammonium ion is removed before tube 8. The resin desorbate in tube 7 shows appreciable ammonium loading while the water in tube 7 shows very little ammonium ion concentration because this is the last tube where ammonium ion was adsorbed onto the resin, and this resin had enough capacity to adsorb the remaining ammonium ion.

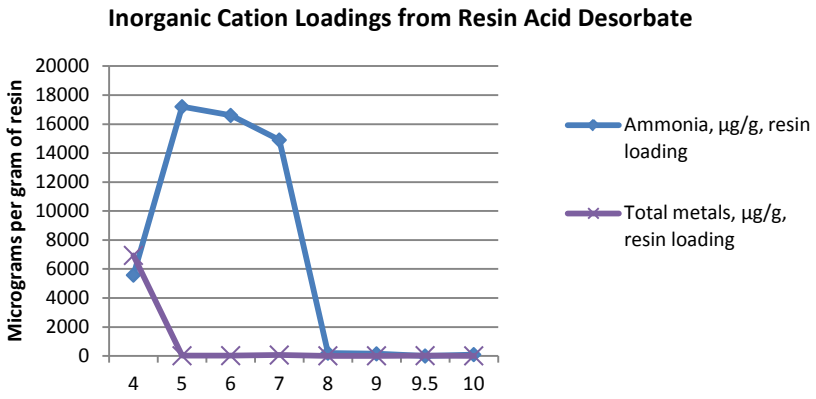

Figure 5. Inorganic cation loading on ion exchange resins (tubes 4-10) as measured in acid desorbate.

Metal cations are measured as total and dissolved metals (mg/L). Total metals are a direct measurement by ICP-OES of the amount of metallic elements in the sample solution and may include particulates. Dissolved metals are measured in the same sample solution after filtering through a 0.2 micrometer filter. Most metals showed little difference in total and dissolved concentrations, except for silver. The total and dissolved concentrations of silver are shown in Figure 6 with turbidity measurements. Water samples from tube 6 and 7 were visually turbid, and measured turbidity values confirmed this. Concentration of total silver and turbidity are both relatively high in tubes 6 and especially 7, and to a lesser degree in tube 9. Turbidity is often caused by organic components and especially by microbial activity and its byproducts. To characterize the source of the turbidity and its relationship to silver content, a comparison to carbon content data and further investigation of the particulates causing the turbidity follows.

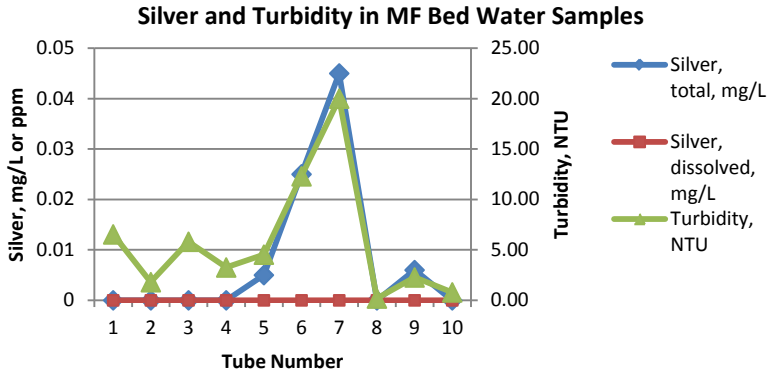

Figure 6. Variation of total and dissolved silver and turbidity in water samples.

Figure 7 is a plot of the measured Total Inorganic Carbon (TIC) and Total Organic Carbon (TOC) values in water from the ten tubes in the MF Bed. TIC stays relatively constant, varying between about 10 and 30 ppm (mg/L of carbon). The TIC in the water is typically carbon dioxide (CO_2), which is present in the water at levels correlating

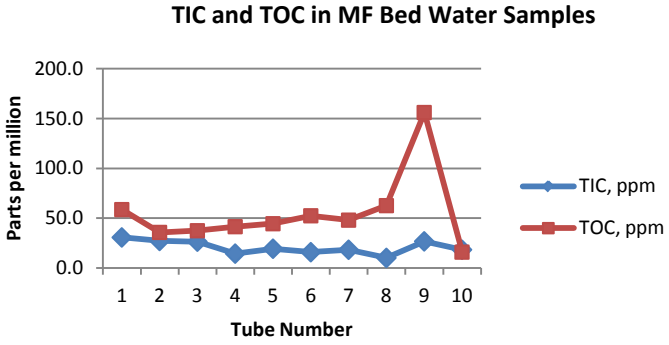

Figure 7. TIC and TOC in MF Bed Water Samples.

to the atmospheric concentration. The TOC, in contrast to the TIC, shows a clear peak in tube 9. As will be discussed in the organics analysis section, the major components of the high TOC measured in tube 9 sample water are N,N-dimethyl-1,2-propanediamine and acetic acid. Although water samples from tubes 6 and 7 were visually turbid and did have high turbidity readings, the TOC for these samples was relatively low. This does not necessarily imply that the source of the turbidity is not organic in nature, however. It is possible that the particulates causing the turbidity, if they do contain carbon, are not easily dissolved or digested during the TOC measurement and are therefore not measured as TOC. This would be the case with microbial detritus. With this as a starting point, we proceeded with analyses designed to characterize the cause of high turbidity in the tube 7 water sample.

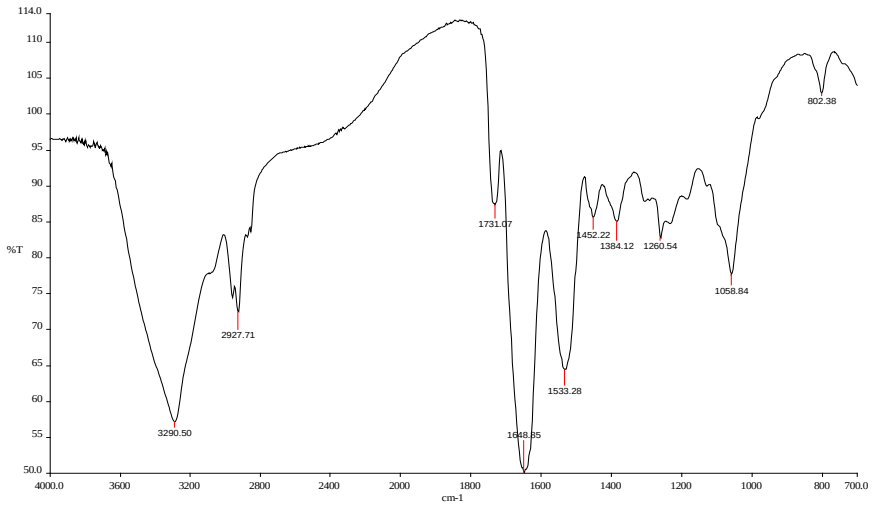

Figure 8. FTIR spectrum of pellet material from tube 7 water sample.

Characterization of Turbidity in Tube 7: To further characterize the particulates causing the turbidity in tube 7, an aliquot of the water was centrifuged at high speed, and the pellet material was collected for Fourier Transform InfraRed (FTIR) spectroscopy and Scanning Electron Microscopy with Energy Dispersive X-Ray Fluorescence detector (SEM/EDXRF). Figure 8 shows the FTIR spectrum of a sample of the pellet isolated from the tube 7 water sample. The spectrum is a good match for proteins. The side carbonyl band at 1731 cm^{-1} has been associated with microbial protein from previous unpublished studies conducted by BHL[2]. The spectrum does not indicate it is derived from biofilm. Past experience with known biofilms has demonstrated very strong, broad absorption peaks for a carbohydrate matrix typical of biofilm in the region of 1000 to 1400 cm^{-1}. Further analyses of the pellet material by SEM/EDXRF (Fig. 9 and 10) show clear evidence of carbon (C), oxygen (O), phosphorus (P), and sulfur (S), which are associated with proteins and other biological detritus. Additionally, a small amount of silver (Ag) is present, confirming the detection of silver by ICP-OES and its association with the turbidity. It is likely that the silver is bound to the predominant protein indicated in the FTIR data. Finally, the spectrum in Figure 10 also indicates the presence of silicon (Si) in the pellet from tube 7, which coincides with the detection of many different silicon containing compounds that are discussed in the organics analysis section.

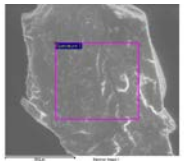

Figure 9. SEM micrograph of particle in pellet material from tube 7 water sample.

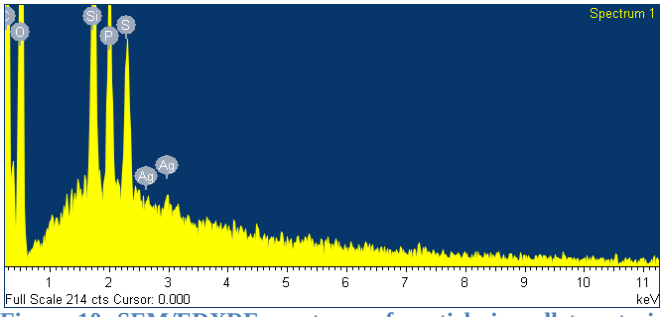

Figure 10. SEM/EDXRF spectrum of particle in pellet material from tube 7 water sample.

The material causing the high turbidity in tube 7 was examined further by staining with crystal violet to allow for visual inspection for the presence of bacteria (Fig. 11). On visual inspection, both large and small particles were seen. The large particles are more predominant and appear to be agglomerations of bacterial detritus containing bacterial rods. Combining this information with that from the FTIR (Fig. 8) and

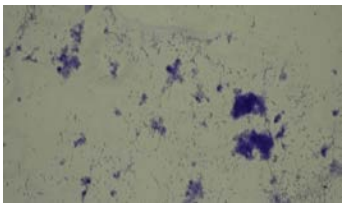

Figure 11. Optical microscope photograph of particulates causing turbidity in tube 7 water sample.

SEM/EDXRF (Fig. 10) spectra, it is likely that the turbidity is primarily due to large particles of insoluble biomass that incorporate the silver and silicon containing compounds. Silver is known to bind to biological compounds. SEM analysis of a swab sample from a film inside tube 7 did show presence of silver, but the ultimate source of the silver and the mechanism by which it was transported to tube 7 is unknown. Although the silicon containing compounds are coincident with the bacteria, the nature of the association between the silicon containing compounds and the bacteria is not known at this time.

Inorganic anions Analysis: Inorganic anion concentrations were measured for both the water samples and the resin basic desorbates. Organic anions (primarily volatile fatty acids) are discussed in the organics analysis sections. Figure 12 shows the anion concentrations for water samples in tubes 1 through 10, and Figure 13 shows the anion loading (mg/g of resin) measured in the basic desorbate from the resin samples in tubes 4 through 10. Most of the inorganic anions are adsorbed on the resin in tube 4. The large amount of phosphate (PO_4^{3-}) and sulfate (SO_4^{2-}) found in the resin sample number 9 (Fig. 13) is actually present from the cation exchange resin in tube 9, and the smaller amount of phosphate (as well as sulfate and chloride) found on the tube 10 resin was likely washed through from tube 9 and readsorbed in tube 10. Figure 14 shows inorganic anion resin loading versus anion type for unused control resins and samples of the flight resin. This allows a comparison of the anions measured in sample resin desorbate to anions measured in control (unused) resin desorbate. Major features of this chart include the chloride and phosphate anion loadings and, to a lesser extent, the sulfate anion loading. Point 1 marks the chloride loading on unused weak base anion exchange resin, which is an unused sample prepared the same way as the second resin in tube 9 of the MF Bed. Point 2 marks the chloride loading of resin from tube 4 in the MF Bed. The measurement of chloride on the tube 4 resin is truly from WPA water and is not an artifact or leachate from the resin itself (because the weak base anion exchange resin is not present in the MF Bed until tube 9). Point 3 marks the phosphate loading on unused the strong cation exchange resin, which is the first resin used in tube 9 of the MF Bed, and Point 4 marks the phosphate loading on unused mixed strong anion/cation exchange resin used in tubes 4 through 8 and tube 10. Additionally, sulfate was also measured on both the strong cation exchange resin and the mixed strong anion/cation exchange resin control samples. Looking again at Figure 13, we can see that the sample from tube 9 (used strong cation exchange resin) has high phosphate and sulfate even though those anions should have been adsorbed on resins in earlier tubes, and the sample from tube 10 (used mixed strong anion/cation exchange resin) has higher phosphate, sulfate and chloride loadings than would be expected. Comparing this with Figure 14, it is apparent that the relatively high phosphate and sulfate loadings in tube 9 were measured because the cation exchange resin in tube 9 is close to its virgin state and was not utilized during the time this MF Bed was in

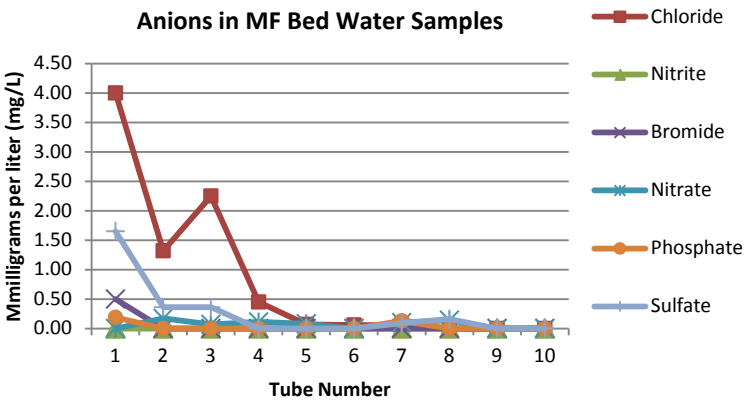

Figure 12. Anion concentration in water from tubes 1 through 10.

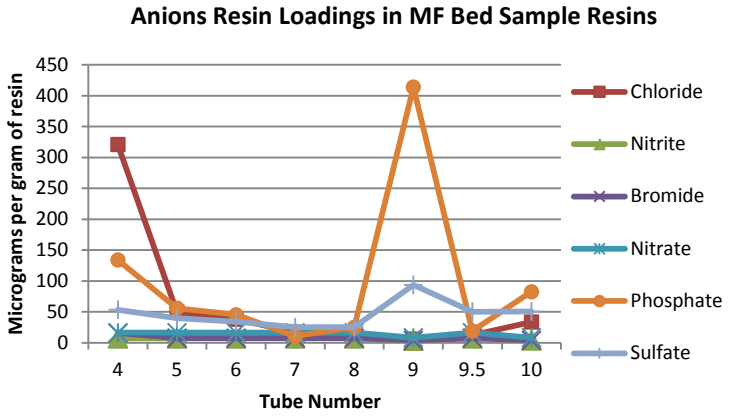

Figure 13. Anion loadings on resin from tubes 4 through 10.

service in the WPA. The relatively high phosphate and sulfate loadings on the resin in tube 10 are likely due to leachates from earlier tubes, but the loadings are still low compared to the capacity of the resin.

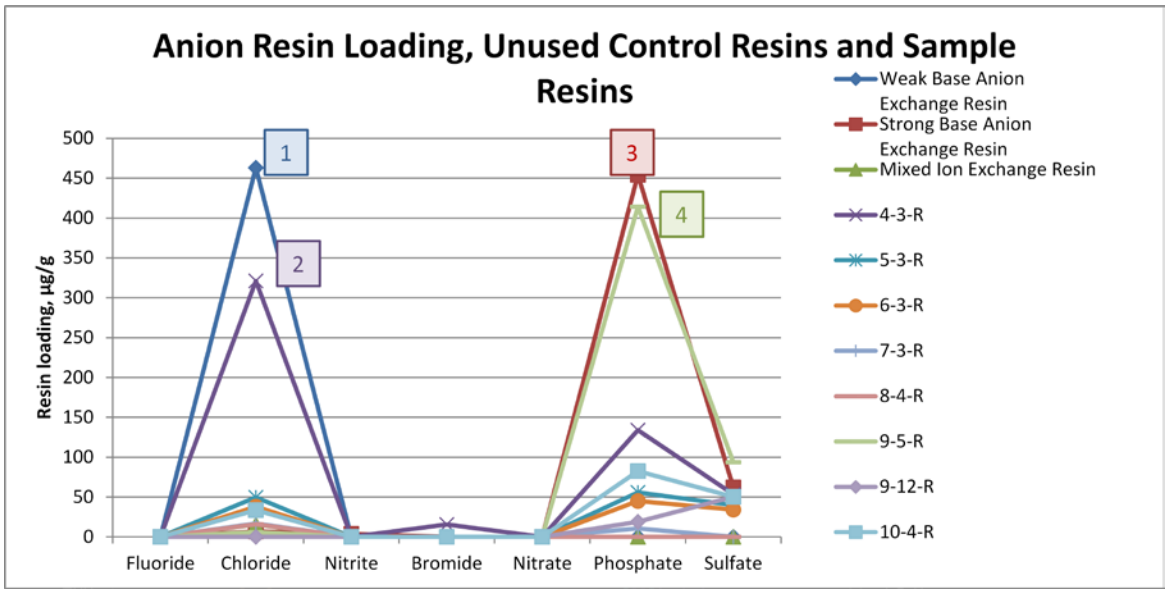

Figure 14. Anion loadings on sample resins and unused control resins.

B. Organics Analysis of Water Samples

Volatile Organic Compounds in Water Samples: Measurement of volatile organic compounds in the MF Bed water samples included both target compounds and tentatively identified compounds. Tentatively identified compounds are identified by their mass spectra and are quantified based on an internal standard while target compounds are identified by their retention time (and confirmed by their mass spectra) and are quantified against a known concentration standard of the same compound. Figure 15 shows the concentration of target volatile compounds (ppb or µg/L) in the water samples from tubes 1 through 10. The main constituents identified are ethanol, acetone, and 2-propanol. Note that dimethylsilanediol (DMSD, which is the source of the anomalous TOC rise that led to the removal of both MF Beds), propylene glycol, and ethylene glycol are also expected at elevated levels throughout the MF Bed, but these organics were not detected with the analytical method used. Because many of the volatiles are not adsorbed by the MF Bed but travel through to be broken down in the Cat Reactor, a somewhat constant

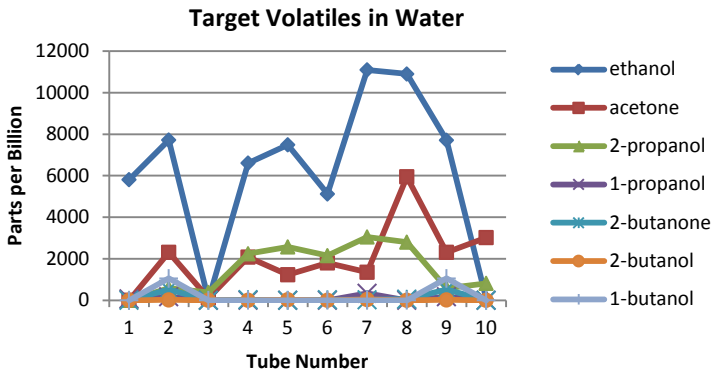

Figure 15. Target volatile concentrations in MF Bed water samples.

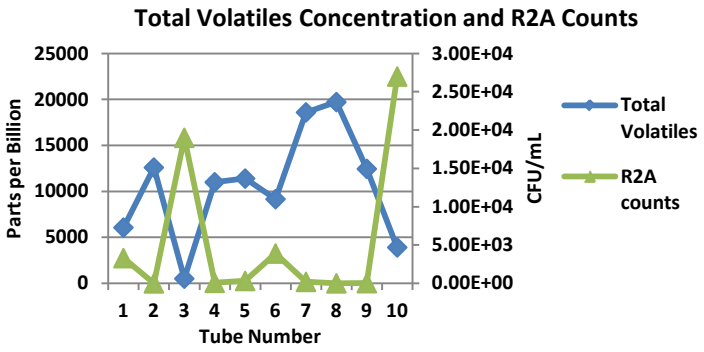

Figure 16. Volatiles and heterotrophic (R2A) microbial counts for MF Bed water samples.

concentration of these compounds throughout all ten tubes would be expected. However, this was not observed. Recall that the MF Bed was stored (both on orbit and on the ground) for many months prior to sampling and analysis. During that time, microbes and fungi could continue to grow and consume the volatile organic compounds. Figure 16 shows the total volatiles concentration and the heterotrophic (R2A) microbial counts versus tube number for all water samples. The tubes with the lowest volatiles concentrations also had the highest heterotrophic (R2A) counts, indicating that the microbes were consuming the volatile compounds during storage.

Along with the target volatile organic compounds, a variety of other compounds were detected, including siloxanes. Siloxanes are organic compounds that include at least one –SiO group and can be made up almost entirely of –SiO groups with organic side chains attached. Silanes also contain silicon (Si) but in –SiH groups instead of being bound to oxygen. Many of the compounds identified were cyclosiloxanes, which are a known breakdown product of polydimethylsiloxane.[2] Figure 17 shows a plot of total volatiles compared to siloxanes in the MF Bed water samples. The scale for volatiles is on the left while the scale for silicon containing compounds is on the right. Although the siloxanes are present in much lower concentrations than other volatile compounds, the trend shows a maximum of siloxane compounds in tube 7. Recall that tube 7 is where the high turbidity biomass was observed condensed into particles that also contain silicon.

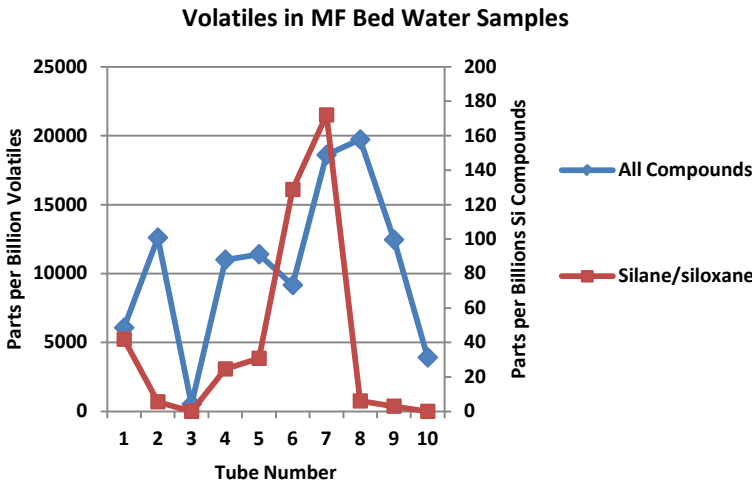

Figure 17. Total volatiles and volatile silane/siloxane compounds in MF Bed water samples.

Semivolatile Organic Compounds in Water Samples: Semivolatile organic compounds were measured in the MF Bed water samples. The semivolatiles are identified based on their mass spectra and retention times and are further classified as amines, acids, silane/siloxanes, or other unclassified compounds. It must be noted here that although the semivolatiles analysis does detect organic acids, it is biased low and will not reflect their true concentration. However, this method does give accurate organic acid trend information from tube to tube. Figure 18 shows the total concentration as well as the concentrations of each class of compounds (silane/siloxane, amine, acid) in the MF Bed water samples. The total concentration decreases through the first three tubes as expected; this is where the carbon adsorbs organic compounds out of the water. There is a low level of organic compound in tubes 3 through 8, and then a very large concentration in tube 9, followed by very low levels in tube 10. The much larger concentration of organic semivolatile compounds in tube 9 is primarily due to one particular compound, N,N-dimethyl-1,3-propanediamine, with a smaller amount of organic acids. The structure of N,N-dimethyl-1,3-propanediamine is shown in Figure 19. Recall that the pH in this water sample is about 6.5. At this pH, both of the amine groups on the N,N-dimethyl-1,3-propanediamine would likely be protonated,

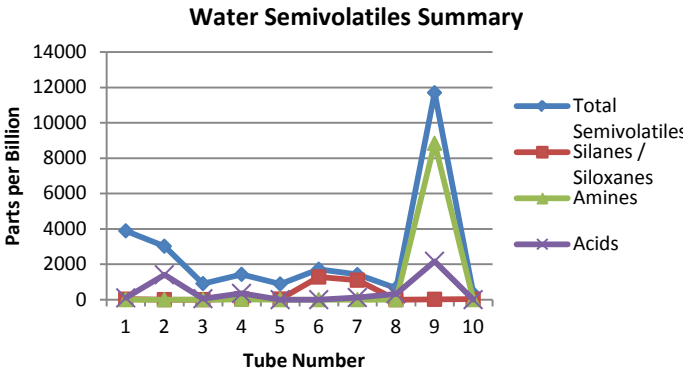

Figure 18. Summary of semivolatiles in MF Bed water samples.

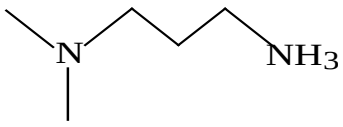

Figure 19. Structure of N,N-dimethyl-1,3-propanediamine.

and this compound would exist as an ion in solution, pairing with organic acids (primarily acetic acid) in their anionic form as a dissolved salt. Amines also act as bases to raise solution pH, so the presence of this diamine contributes to the raised pH in tube 9. Also recall that the conductivity was highest in tube 9, which is partially due to the presence of the diamine compound in its ionic form (the presence of organic acids also contributes to the high conductivity). It would be highly unlikely for N,N-dimethyl-1,3-propanediamine to have migrated through the MF Bed all the way to tube 9 without being adsorbed onto the ion exchange resins. Instead, it has been produced in tube 9 through the breakdown of the weak base ion exchange resin filling the second half of tube 9. The organic acid concentration is also relatively high in tube 9, but more accurate organic acid concentration data is found in the discussion of the volatile fatty acid analysis. Also notable in the semivolatiles analysis data is the presence of silicon containing compounds, primarily siloxanes, in tubes 6 and 7. In fact, siloxanes make up almost all of the semivolatile compounds detected in tubes 6 and 7. This coincides with the siloxane peak observed in the volatiles analysis. Finally, the very low level of semivolatiles in tube 10 indicates that, during use, semivolatile organic compounds were adsorbed by resins prior to tube 10. The MF Bed was functioning well with respect to semivolatile compounds.

Volatile Fatty Acids (VFA) in Water Samples: Volatile fatty acids include organic acids with one to seven carbons. While these acids are individually quantified, it is useful to look at the total and the major contributing compounds. Figure 20 shows the total VFA concentration and the acetic acid concentration (both in mg/L) for the MF Bed water samples. With the exception of tube 1 (see carbon resin analysis) and tube 7, by far the predominant acid is acetic acid. Acetic acid is an end product of the metabolism of organic acids. In tube 1, formic acid is present (another end product of organic acid digestion), and in tube 7, formic and butyric acids are present as well as acetic acid.

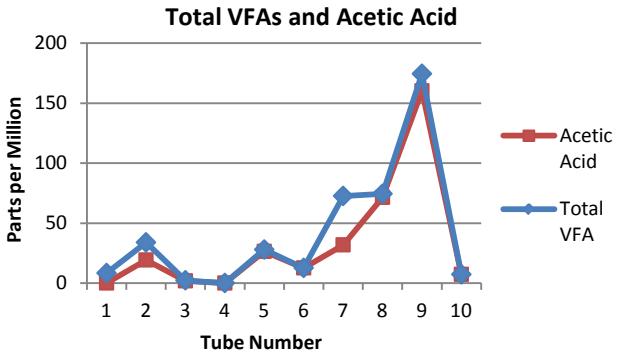

Figure 20. Total VFAs and acetic acid concentration in MF Bed water samples.

C. Organics Analysis of Sorbent (Resin) Samples

Carbon Resin Loading, Semivolatile Organic Compounds: Carbon sorbent loadings were determined by desorbing ~5 g carbon samples with pure methanol, a methanol / dichloromethane mix, and finally with pure dichloromethane. The resulting desorbate was then analyzed by GC-MS. The total semivolatiles loading on the carbon resin (milligrams per gram of resin) is shown in Figure 21, along with the loading of silane and siloxane compounds for the first three tubes. Clearly, the carbon resin in the first tube sorbed a large mass of compounds, and the carbon resin in the second and third tubes have plenty of capacity left, so the MF Bed was not overloaded with respect to the carbon resin capacity. Three compounds made up over 75% of the mass loaded on the carbon resin in the first tube: hexanoic acid, benzoic acid, and caprolactam as can be seen in the chromatogram in Figure 22. Hexanoic acid and benzoic acid are metabolic byproducts. Caprolactam is a monomer used in the production of Nylon 6® and has been consistently measured in humidity condensate.[2] Caprolactam is a byproduct from Nylon® Velcro, which is used extensively on ISS. The siloxane compounds detected in the carbon sorbent desorbates include tentatively identifiable long chain and cyclic compounds as well as many unidentified, but classifiable, compounds. Siloxanes have a very recognizable mass spectral signature. Even though many of the siloxanes are not found in the mass spectrum search libraries, they can still be identified as siloxane or silane type compounds. The silane/siloxane loading, while much less than the loading of other compounds in tube 1, makes up about 35% to 40% of the loading

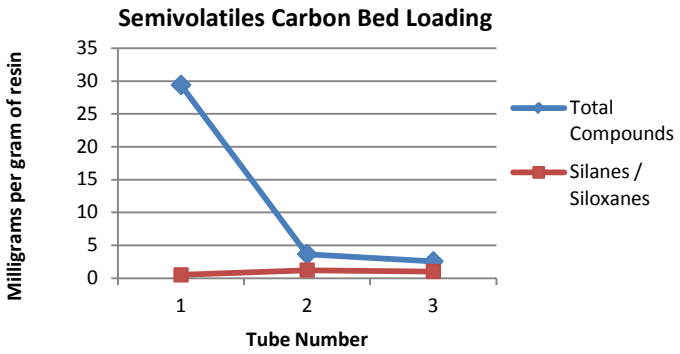

Figure 21. Loading (mg/g) of semivolati`le compounds on carbon sorbent samples from tubes 1 through 3.

on carbon resins in tubes 2 and 3 (Fig. 21). The loading does not change much from tube 2 to tube 3, despite the fact that there are still siloxanes present further downstream in the MF Bed as seen in water and resin analyses previously discussed (Fig. 17 and 18). It is evident that the carbon resins do not adsorb siloxanes strongly enough to prevent their passage through the MF Bed.

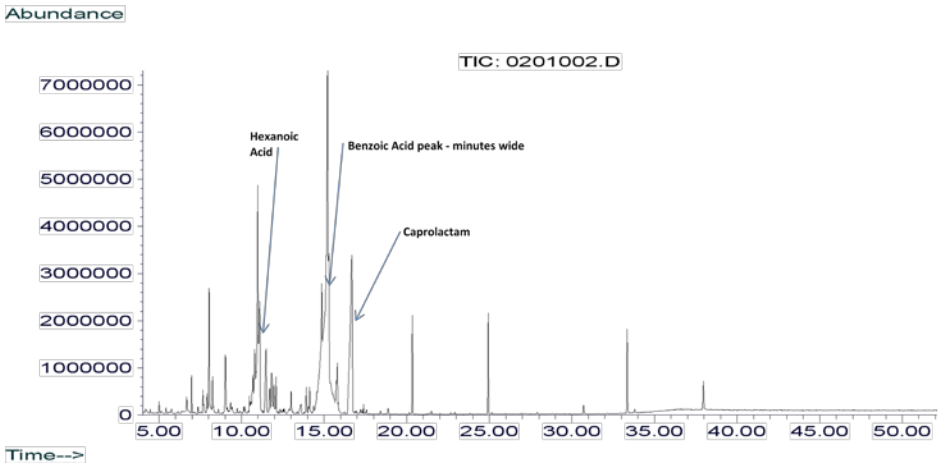

Figure 22. Total ion chromatogram (TIC) for desorbate from carbon sample from tube 1.

Ion Exchange Resin Loading, Semivolatile Organic Compounds: The ion exchange resins were desorbed as described in Figure 2 and the desorbate analyzed by GC-MS. Figure 23 shows the resin loading as measured in the base desorbate, base / neutral extract. The resins were desorbed with 0.5 N NaOH, and the desorbate was extracted with dichloromethane (removing basic and neutral compounds into the extract), and the extract was reduced and analyzed for semivolatiles. The data show that the total loading is uneven; although the loading on the resin in tube 4 is highest, there are two other peaks in resin loading, in tube 7 and in the first resin in tube 9. Examining different classes of compounds (silane/siloxanes, amines, and acids) will help to better understand the total loading data. First, consider the silane/siloxane group of compounds, represented by the red line. As in the water analysis data, these compounds peak in tubes 6 and 7, and are, in fact, the great majority of compounds identified in the analysis of tube 6 and 7 resin desorbates. After tube 7, the silane/siloxane loading is very low in comparison. Next, consider amines, represented by the green line, which are readily adsorbed by the resin in tubes 4 and 5 with very little loading after that until the resin samples from tubes 9 and 10. Unlike the other tubes in the MF Bed, there are two separate resins loaded into tube 9. The first resin (in terms of water flow) in tube 9 is a strong cation exchange resin, and the second is a weak base anion exchange resin. The same compound identified in the tube 9 water semivolatile analysis (N,N-dimethyl-1,3-propanediamine) is the main amine identified on the resins from tubes 9 and 10. As the weak base anion exchange resin breaks down, the diamine in its cation form will be adsorbed by the strong cation exchange resin in the same tube. There is also a lesser amount of the diamine (about half that on the strong cation exchange resin) on the weak base anion exchange resin. It is likely that the diamine is adsorbed by weak base anion exchange resin is part of an ion pair with acetic acid in its acetate ion form. The N,N-dimethyl-1,3-propanediamine is also present on tube 10 resin due to resin degradation before and during use in the WPA. Flow through the MF Bed carried the diamine into tube 10 where it was adsorbed by the ion exchange resin. Note

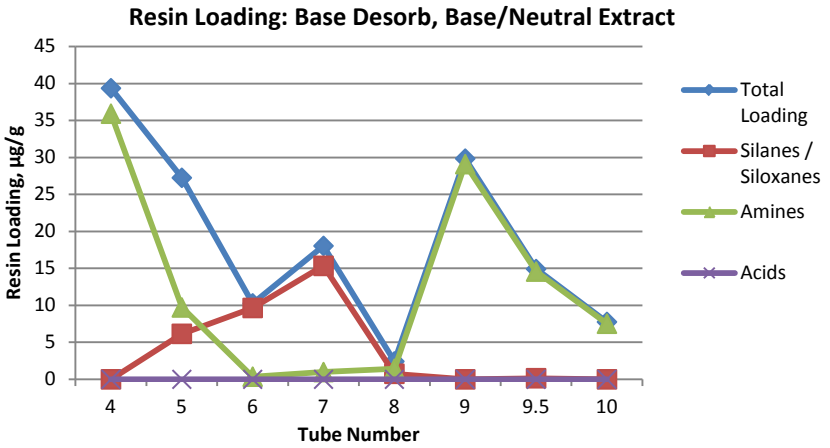

Figure 23. Resin loading for semivolatile organic compounds measured in base desorbate, base / neutral extract of samples from tube 4 through 10.

that the loading in tube 10 is only about 8 µg/g and does not significantly impact the capacity of the resin. Finally, we see that the acid loading is very low for the base desorbate, base / neutral extraction, as would be expected.

The base desorbate, acid / neutral extract data are shown in Figure 24, with the same classes of compounds. Again, there is a peak of silane/siloxane compounds on the resins from tubes 6 and 7. The primary compounds identified in this analysis were acids, represented by the purple line, that were adsorbed on the resin in their anionic form. Although more accurate organic acid concentrations are found in the VFA analysis results, trend indications can be seen in the data here. The primary feature is the peak loading for organic acids on the weak base anion exchange resin in tube 9, which was chosen specifically for its ability to retain acetic acid (acetate ion form). The very low acid loading on the resin in tube 10 is also notable. Together, these two measurements show that the MF Bed design was very effective in removing VFAs (specifically, acetic acid).

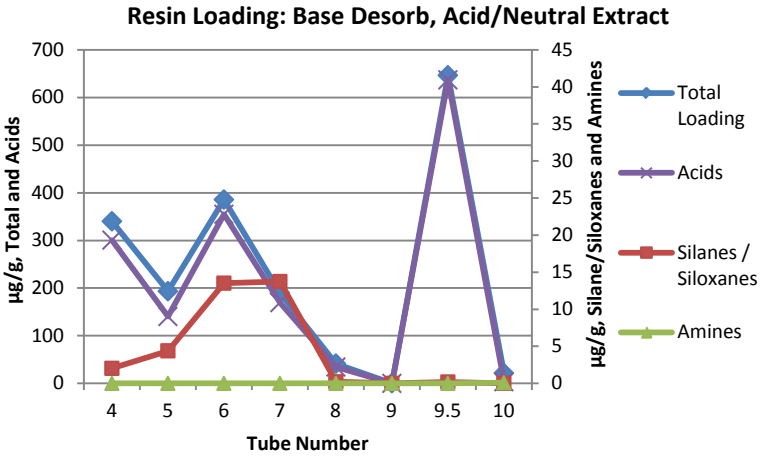

Figure 24. Resin loading for semivolatile organic compounds measured in base desorbate, acid/ neutral extract of samples from tube 4 through 10.

Data from the acid desorbate, acid / neutral extraction are shown in Figure 25. Again, we see a peak in siloxane loading in tube 7, although the siloxanes (right hand scale) are a small portion of the total resin loading (left hand scale). Organic (fatty) acids are the major components recovered from resin desorption. Note that the resin from tube 10 is very clean.

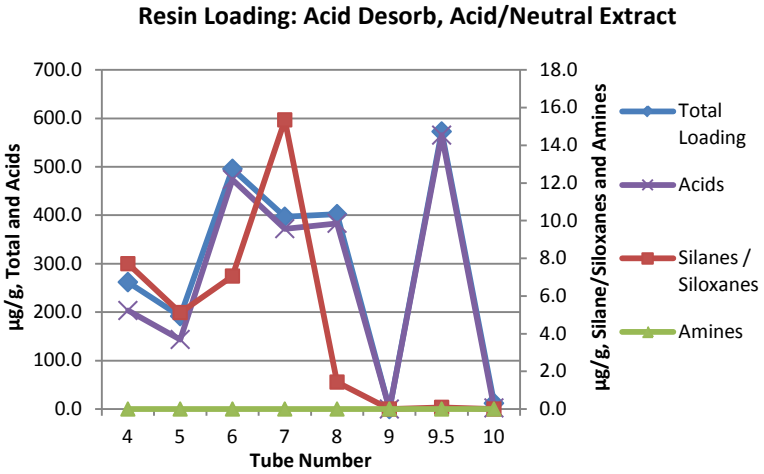

Figure 25. Resin loading for semivolatile organic compounds measured in acid desorbate, acid / neutral extract of samples from tube 4 through 10.

Figure 26 shows the summary data from the acid desorbate, base / neutral extraction. The total resin loading in these samples is much less than in the other three fractions. The major components are amines and silane/siloxanes, with the silane/siloxanes peaking in tube 7, as with other fractions.

Each desorbate and extraction combination is designed to separate compounds with different pH dependent properties (acid or base character). Because siloxanes and silanes are effectively neutral with respect to pH, we would expect their loading to be equal regardless of the

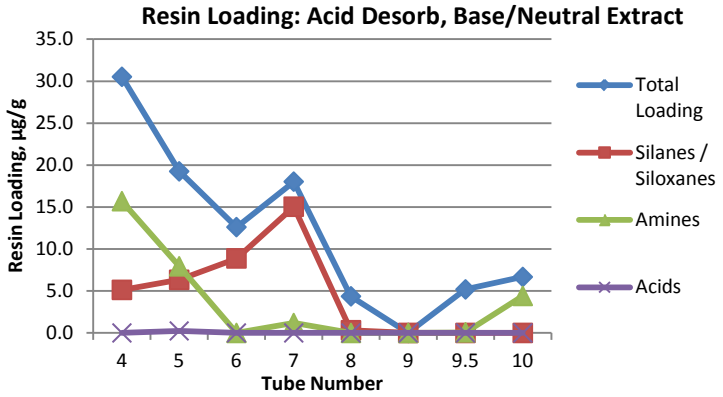

Figure 26. Resin loading for semivolatile organic compounds measured in acid desorbate, base / neutral extract of samples from tube 4 through 10.

way in which they were isolated. Figure 27 shows a plot of silane/siloxane loadings from all four different desorbate extractions. The profiles are similar but not identical; differences may be due to competition for sorbent sites on the resins as well as subtle differences in the pH dependent behavior of the specific silane/siloxane compounds. Despite the variation in data from tubes 4 and 6, the silane/siloxane loading peaks in tube 7, which is consistent across water and resin samples, volatiles and semivolatiles analyses, and is coincident with the maximum count for heterotrophic bacterial growth. As previously stated, the reason for the correlation between silane / siloxane compounds and bacterial growth is not known at this time.

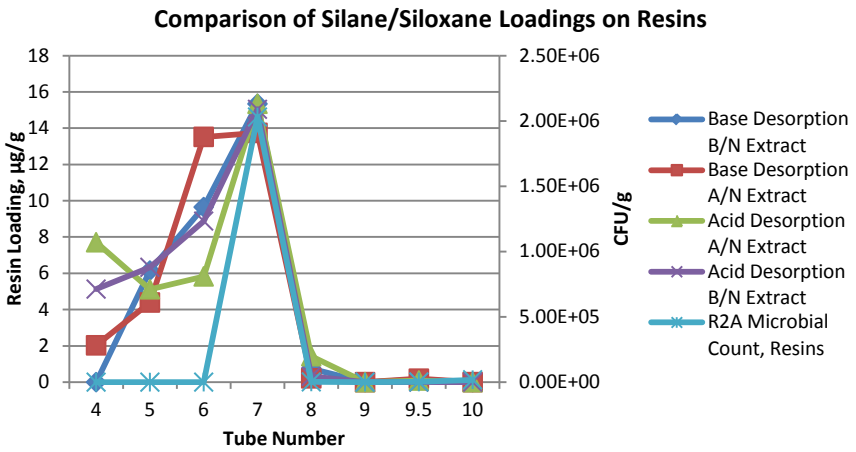

Figure 27. Comparison of resin loadings for silanes / siloxanes measured in all four desorbate extracts of samples from tube 4 through 10 with heterotrophic (R2A) microbial counts from resin samples.

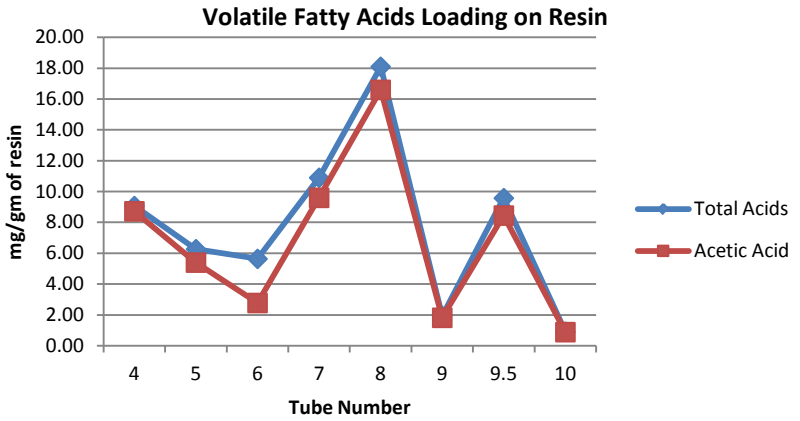

Figure 28. Resin loading for volatile fatty acids on resin samples.

Volatile Fatty Acids (VFAs) Resin Loading: The data shown in Figure 28 summarize the total VFA resin loadings and acetic acid loadings as measured in acidified base desorbate. Unlike the semivolatile analysis, the VFA analysis is done via direct injection and does not require extraction. With the exception of resin from tube 6, acetic acid is the major component. Formic, propanoic, isobutyric, and butyric acids make up the remainder of the total loading with acetic acid on the resin from tube 6. Figure 29 compares the total VFA results from both the water samples and the resin samples. Note that resin sample 9 (strong cation exchange resin) has a low VFA loading while resin sample 9.5 (weak base anion exchange resin) has a higher VFA loading. As previously noted, it is likely that ion pairs of N,N-dimethyl-1,3-propanediamine and acetate ion are adsorbed on these resins. Tube 10 has the lowest measured VFA resin loading and a low VFA water concentration, indicating that the VFAs (with acetic acid predominating) are adsorbed well by the previous resins. Although the weak base anion exchange resin is clearly degrading based on the presence of N,N-dimethyl-1,3-propanediamine, it is also adsorbing acetic acid very well, as it is intended to. With respect to the degradation of the anion exchange resin in tube 9, it is important to note that the timing of the degradation is unclear. There is evidence of some

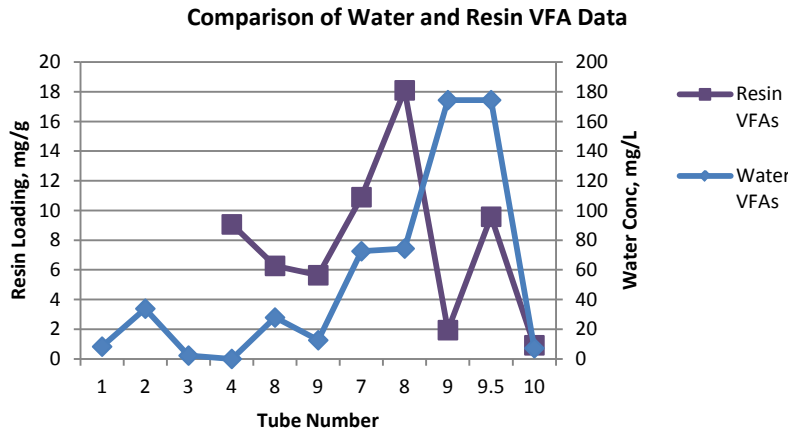

Figure 29. Water and resin loading comparison of VFA data.

degradation prior to or during use (presence of N,N-dimethyl-1,3-propanediamine on tube 10 resin). There is strong evidence of degradation during storage after use (presence of N,N-dimethyl-1,3-propanediamine in tube 9 water and on strong cation exchange resin from tube 9).

D. Microbiological Analyses

The enumeration and identification of heterotrophic bacteria from carbon and resins is provided in Table 3. The relative species counts based on the totals for each specific colony morphology on countable plates are provided following the species identification.

Table 3. Enumeration and identification of heterotrophic bacteria from carbon and resins.

Tube Number	Sample	Bacteria Count CFU/g	Bacteria Identifications
1	Activated Carbon	3.00E+04	*Ralstonia pickettii* – 2.55E+04 CFU/g
			Cupriavidus metallidurans – 4.50E+03 CFU/g
2	Activated Carbon	1.01E+05	Unidentified GNR (low match *Bradyrhizobium*/*Phyllobacterium*) – 9.47E+04 CFU/g
			Cupriavidus metallidurans – 6.31E+03 CFU/g
3	Activated Carbon	2.00E+04	Unidentified GNR (low match *Bradyrhizobium*/*Phyllobacterium*) – 1.81E+04 CFU/g
			Bradyrhizobium japonicum – 1.90E+03 CFU/g
4	Mixed strong ion exchange resin	1.53E+02	*Ralstonia pickettii* – 1.53E+02 CFU/g
5	Mixed strong ion exchange resin	49	*Ralstonia pickettii* – 43 CFU/g
			Unidentified GNR (low match *Flavobacterium*) – 6 CFU/g
6	Mixed strong ion exchange resin	2.42E+02	*Ralstonia pickettii* 2.07E+02 CFU/g
			Unidentified GNR (low match *Flavobacterium*) – 35 CFU/g
7	Mixed strong ion exchange resin	2.03E+06	*Burkholderia cepacia* – 1.96E+06 CFU/g
			Burkholderia cenocepacia – 7.00E+04 CFU/g
8	Mixed strong ion exchange resin	1.84E+03	*Burkholderia cepacia* – 1.70E+03 CFU/g
			Ralstonia pickettii – 1.40E+02 CFU/g
9	Strong cation exchange resin	2.13E+02	*Burkholderia cepacia* – 1.67E+02 CFU/g
			Burkholderia cenocepacia – 46 CFU/g
9	Weak anion exchange resin	1.33E+03	*Burkholderia cepacia* – 1.30E+03 CFU/g
			Burkholderia cenocepacia – 30 CFU/g
10	Mixed strong ion exchange resin	1.84E+04	*Burkholderia cepacia* – 1.58E+04 CFU/g
			Burkholderia cenocepacia – 2.60E+03 CFU/g

The enumeration and identification of heterotrophic bacteria in water is shown in Table 4. The relative species counts based on the totals for each specific colony morphology on countable plates are provided following the species identification.

Table 4. Enumeration and identification of heterotrophic bacteria in water.

Tube Number	Sample	Bacteria Count CFU/mL	Bacteria Identifications
1	Water	3.3E+03	*Bradyrhizobium japonicum* – 3.02E+03 CFU/mL
			Unidentified GNR (low match *Bradyrhizobium*/*Phyllobacterium*) – 2.80E+02 CFU/mL
2	Water	<10	
3	Water	1.9E+04	*Bradyrhizobium japonicum* – 1.63E+04 CFU/mL
			Unidentified GNR (low match *Bradyrhizobium*/*Phyllobacterium*) – 2.70E+03 CFU/mL
			Ralstonia pickettii – Isolated from TNTC plate
4	Water	7.4E+01	*Bradyrhizobium japonicum* – 66 CFU/mL
			Ralstonia pickettii – 8 CFU/mL
			Burkholderia cepacia – Isolated from TNTC plate
5	Water	3.2E+02	*Ralstonia pickettii* – 1.69E+02CFU/mL
			Cupriavidus metallidurans - 1.41E+02 CFU/mL
			Unidentified GNR (low match *Flavobacterium*) – 9 CFU/mL
6	Water	3.9E+03	*Ralstonia pickettii* – 3.9E+03 CFU/mL
			Burkholderia cepacia – Isolated from TNTC plate
			Unidentified GNR (low match *Flavobacterium*) – Isolated from TNTC plate
7	Water	2.0E+02	*Burkholderia cepacia* – 1.33E+02 CFU/mL
			Burkholderia cenocepacia – 6.07E+03 CFU/mL
8	Water	<10	
9	Water	3.7E+01	*Ralstonia pickettii* – 24 CFU/mL
			Unidentified GNR (low match *Flavobacterium*) – 9 CFU/mL
			Burkholderia cenocepacia – 4 CFU/mL
10	Water	2.7E+04	*Ralstonia pickettii* – 2.48E+04 CFU/mL
			Burkholderia cepacia – 2.20E+03 CFU/mL
			Burkholderia cenocepacia – Isolated from TNTC plate

The bacteria present on the carbon, resins, and in the water drained from the multifiltration beds are Gram negative species commonly found in wastewater, soil, and deionized water. Several species of rod-shaped, motile, Gram negative, aerobic, and non-fermentative bacteria were present including *Ralstonia pickettii*, *Cupriavidus metallidurans*, Ralstonia *paucula*, *Bradyrhizobium japonicum*, Burkholderia *cepacia*, *Burkholderia cenocepacia*, an unidentified Gram negative rod-shaped bacterium similar to *Bradyrhizobium* and *Phyllobacterium* and an unidentified Gram negative rod-shaped bacterium similar to *Flavobacterium*. *Ralstonia pickettii* is commonly found in biofilms in water systems and can cause nosocomial infections in immune compromised individuals.[5] *Cupriavidus metallidurans* has the ability to survive in millimolar concentrations of heavy metals.[6] *Burkholderia cepacia* is resistant to several antimicrobials including iodine which is the disinfectant used in the United States water processor assembly on the International Space Station.[7] *Burkholderia cenocepacia* is a subspecies of *Burkholderia cepacia* and is an opportunistic pathogen and human infections are common in patients with cystic fibrosis and chronic granulomatous disease.[8] *Bradyrhizobium japonicum* is a soil bacterium from the family *Rhizobiaceae*. *Bradyrhizobium* is present in plant root nodules including soybeans and is involved in fixing atmospheric nitrogen into combined forms utilizable by the host plant.[9] The colony morphology of the unidentified Gram negative rod-shaped bacterium similar to *Bradyrhizobium and Phyllobacterium* is light beige to gray, punctiform, and round. The colony morphology of the unidentified Gram negative rod-shaped bacterium similar to *Flavobacterium* is opaque, glossy, irregular shaped with a burnt orange pigmentation.

No fungi were present in the water or on the carbon and resins. The count for fungi in water samples from all 10 tubes was <1 CFU/mL. The count for fungi on activated carbon and resins was <10 CFU/g.

V. Conclusion

Chemical analysis of inorganic and organic compounds in water and on resin samples from MF Bed S/N 00003 confirm that there is remaining capacity for cations and organic compounds on the various adsorbent media. Based on the data available, bicarbonate (predominant form dissolved CO_2 at the measured pH) had initially saturated the MF Bed and was present in the effluent. The weak base anion exchange resin in tube 9 that was chosen for its ability to adsorb acetic acid performed well despite some degradation, including evidence of further degradation after the MF Bed was taken out of service. Tube 7, where siloxane compounds were observed, remains an anomaly and demonstrates that silanes and siloxanes can pass through the MF Bed unadsorbed. In fact, these analyses show that various siloxanes were not effectively removed by the adsorbent in the MF Beds and appeared to have saturated the entire MF Bed. Since these siloxanes will eventually reach the Catalytic Reactor, modifications to the MF Bed will likely be required to remove these problematic organics.

Heterotrophic bacteria counts on activated carbon and resins ranged from <10 CFU/g to 2.03E+06 CFU/g. These levels of attached bacteria were lower than expected and there was no visible evidence of microbial mats which could occlude flow through the sorbents. The bacterial counts in water ranged from <10 CFU/mL to 2.7E+04 CFU/mL. Overall, the planktonic population of bacteria was lower than expected and fungi were not present. Some variability in bacterial concentrations may be due to settling of bacteria to one end of the tubes which were stored vertically. Additional variation from tube to tube may be due to approximately 1 year of stagnant storage prior to analysis, pH, chemical constituents on carbon and resins, and chemical constituents in the water. For instance, the pH drop after tube 6 due to disappearance of the ammonium ion coupled with increasing concentrations of organic acids and volatile fatty acids in tubes 7 and 8 shifted the predominant species to *Burkholderia cepacia* and *Burkholderia cenocepacia*. These bacterial species and levels are not unexpected in the WPA MF Beds and are readily removed by the Catalytic Reactor located downstream.

Acknowledgments

The work described in this paper was performed by NASA, Boeing, and Hamilton Sundstrand Space Systems International, Inc. under the auspices of the International Space Station contract, NAS15-10000. The authors wish to express their sincere thanks to Natalee Weir of Boeing for the microbiological analyses,to Eric Cramblit and Sam Manuel of Boeing for their chemical analyses, and to Joyce Carpenter, Robert Meskill, and Wayne Kloter of Hamilton Sundstrand for their support.

References

[1]Carter, D.L., N. Orozco, "Status of the Regenerative ECLSS Water Recovery System", AIAA 1021863, presented at the 41st International Conference on Environmental Systems, Portland, Oregon, July, 2011.

[2]Clarson, S. J., and Semlyen, J. A., *Siloxane Polymers*, P T R Prentice Hall, Inc., New Jersey, 1993, Chaps. 7.

[3]Previous work at Boeing Huntsville Laboratory, unpublished.

[4]*Standard Methods for the Examination of Water and Wastewater 17th ed.*, edited by L. S. Clesceri, A. E. Greenberg, and R. R. Trussell, American Public Health Association, Washington, DC, 1989.

[5]Vandamme, P., Goris, J., Coenye, T., Hoste, B., Janssens, D., Kersters, K., De Vos, P., and Falsen, E., "Assignment of Centers for Disease Control group IVc-2 to the Genus *Ralstonia* as *Ralstonia paucula* sp. nov.," Int. J. Syst. Bacteriol., Vol. 49, 1999, pp. 663-669.

[6]Vaneechoutte, M., Kämpfer, P., De Baere, T., Falsen, E., and Verschraegen, G.,"*Wautersia* gen. nov., a Novel Genus Accomodating the Phylogenetic Lineage Including *Ralstonia eutropha* and Related Species, and Proposal of *Ralstonia* [*Pseudomonas*] *syzygii* (Roberts et al. 1990) comb. nov.," Int. J. Syst. Evol. Microbiol., Vol. 54, 2004, pp. 317-327.

7Anderson, R., Vess, R., Panlilio, A., and Favero, M., "Prolonged Survival of *Pseudomonas cepacia* in Commercially Manufactured Povidone-Iodine", Appl. Environ. Microbiol. 56 (11), 1990, pp. 3598 - 3600.

8Mahenthiralingam, E. and Vandamme, P., "Taxonomy and Pathogenesis of the *Burkholderia cepacia* Complex," Chron Respir Dis 2 (4), 2005, pp. 209–217.

[9]*Bergey's Manual of Determinative Bacteriology Ninth Ed.*, edited by J. G. Holt, N. R. Krieg, P. H. A. Sneath, J. T. Staley, and S. T. Williams, Williams & Wilkins, Baltimore, 1994, p. 78.